

Negative terahertz conductivity at vertical carrier injection in a black-Arsenic-Phosphorus-Graphene heterostructure integrated with a light-emitting diode

Victor Ryzhii^{1,2,3,4}, Maxim Ryzhii⁵, Taiichi Otsuji¹, Valery E. Karasik⁴,
Vladimir G. Leiman⁵, Vladimir Mitin⁶, and Michael S. Shur⁷

¹*Research Institute of Electrical Communication,
Tohoku University, Sendai 980-8577, Japan*

²*Institute of Ultra High Frequency Semiconductor Electronics of RAS,
Moscow 117105, Russia*

³*Center for Photonics and Infrared Technology,
Bauman Moscow State Technical University,
Moscow 111005, Russia*

⁴*Center for Photonics and Two-Dimensional Materials,
Moscow Institute of Physics Technology,
Dolgoprudny 141700, Russia*

⁵*Department of Computer Science and Engineering,
University of Aizu, Aizu-Wakamatsu 965-8580, Japan*

⁶*Department of Electrical Engineering,
University at Buffalo, SUNY,
Buffalo, New York, 1460-1920 USA*

⁷*Department of Electrical,
Computer, and Systems Engineering,
Rensselaer Polytechnic Institute,
Troy, New York 12180, USA*

Key words - Black arsenic-phosphorus, graphene, integration with light-emitting diode, injection, carrier cooling, terahertz lasing.

We propose and analyze the heterostructure comprising a black-arsenic-phosphorus layer (b-As_{1-x}P_xL) and a graphene layer (GL) integrated with a light-emitting diode (LED). The integrated b-As_{1-x}P_xL-GL-LED heterostructure can serve as an active part of the terahertz (THz) laser using the interband radiative transitions in the GL. The feasibility of the proposed concept is enabled by the combination of relatively narrow energy gap in the b-As_{1-x}P_xL and the proper band alignment with the GL. The operation of the device in question is associated with the generation of the electron-hole pairs by the LED emitted near-infrared radiation in the b-As_{1-x}P_xL, cooling of the photogenerated electrons and holes in this layer, and their injection into the GL. Since the minimum b-As_{1-x}P_xL energy gap ($\Delta_G \simeq 0.15$ eV) is smaller than the energy of optical phonons in the GL, ($\hbar\omega_0 \simeq 0.2$ eV), the injection into the GL can lead to a relatively weak heating of the two-dimensional electron-hole plasma (2D-EHP) in the GL. At the temperatures somewhat lower than the room temperature, the injection can cool the 2D-EHP. This is beneficial for the interband population inversion in the GL, reinforcement of its negative dynamic conductivity, and the realization of the optical and plasmonic modes lasing supporting the new types of the THz radiation sources.

I. INTRODUCTION

The gapless energy spectrum of graphene layers (GLs) [1] supporting the terahertz (THz) and far-infrared (FIR) radiative interband transitions enables the detection, control, and generation of the THz and FIR radiation (see, for example, the review articles [2–6] and the references therein). One of the most interesting potential application of the GLs and the GL-based heterostructures is their use in efficient THz and FIR lasers that were predicted to operate at room temperature and already demonstrated operation at 100 K [7–20]. Such lasers can be particularly useful in the spectral range below 5 to 10 THz where the operation of the heterostructure lasers based on A₃B₅ compounds is hampered by a strong radi-

ation absorption by the optical phonons. Both the optical and injection pumping of GL-based heterostructures can lead to the interband population inversion and enable the negative dynamic conductivity in the THz and FIR spectral ranges. The quantum efficiency of the optical pumping into the GLs is limited by relatively low absorption coefficient of the GLs ($\beta = \pi\alpha \simeq 0.023$, where $\alpha = e^2/\hbar c \simeq 1/137$ is the fine structure constant, e is the electron charge, \hbar is the reduced Planck constant, and c is the speed of light in vacuum). Apart from this, the generation of the electron-hole pairs in the GL by the near- and mid-infrared (NIR and MIR) photons, i.e., by the photons with relatively high energy can lead to a substantial heating of the two-dimensional electron-hole plasma (2D-EHP) in the GL. This is because, the ini-

tial energy, ε_0 , of the electrons and holes generated by the incident NIR photons ($\varepsilon_0 = \hbar\Omega/2$, where $\hbar\Omega \sim 1$ eV is the photon energy of the pumping radiation). As a result, the effective temperature of the 2D-EHP could be rather large. This complicates the achievement of the interband population inversion in the GLs [22]. The low absorption limitation can be partially avoided in the heterostructures including multiple non-Bernal stacked GLs [9]. The quantum efficiency of the optical pumping can be enhanced, for example, by using a bulk absorption layer, in which the incident NIR/MIR radiation with the photon energy $\hbar\Omega$ exceeding the energy gap of this layer Δ_G generates the electron-hole pairs followed by their vertical diffusion into the GL [21] (perpendicular to the GL plane). However, in the case of the GaAs (or similar materials) as the absorption layer [21], although the pumping quantum efficiency can be markedly increased, the injected electrons and holes are still fairly hot, because the carriers are injected into the GL still with a high energy $\varepsilon_i \gtrsim \Delta_G \sim 1$ eV. In principle, the GL optical pumping by “warm” carriers can be realized using the CO₂ or mid-infrared (MIR) quantum cascade lasers. But the optical pumping by NIR/MIR light-emitting diodes (LEDs) or lasers appears to be much more practical.

In this paper, we propose to use for the GL-based THz and FIR lasers the absorption layer with the sufficiently narrow energy gap and the proper band alignment with the GL [23–27]. As for the material for such a layer can be chosen black-arsenic-phosphorus (b-As_{1-x}P_x) or black-arsenic (b-As). The b-As_{1-x}P_x layer comprising a relatively large number of the atomic sheets can exhibit the energy gap $\Delta_g \simeq 0.15$ eV when the phosphorus fraction x is small [28–31] (at $x = 0.17$, i.e., close to b-As). Further decrease in x , i.e., up to pure b-As may push the band gap to even smaller values [28]. In the case of the b-As_{1-x}P_x absorbing layer, the optical pumping can be provided by a source of NIR/MIR radiation as previously, but due to an effective cooling of the generated and propagated carriers in this layer, their energy of the injected pair being about Δ_G can be much smaller than $\hbar\Omega$. Thus, the absorption layer with relatively narrow energy gap can play an extra role of the carrier cooler. Such a combination can enable both the realization of a high pumping quantum efficiency and the injection of “warm” carriers. As show in the paper, the injection into the GL of the carriers with the energy smaller than the energy of optical phonons in the GL $\hbar\omega_0 \simeq 0.2$ eV can result in the 2D-EHP strong cooling. The latter reinforces the interband population inversion in the GL and the effect of its negative dynamic conductivity. Recent advances in the b-As_{1-x}P_x-based heterostructure fabrication (see, for example, [29–32] are in favor of the feasibility of the proposed lasers.

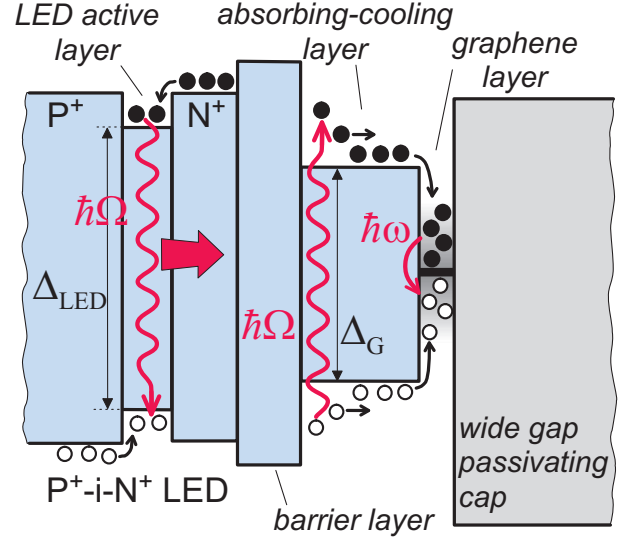


FIG. 1: Schematic view of the band diagram of a b-As_{1-x}P_x-GL heterostructure integrated with a P⁺-i-N⁺-LED (at sufficiently strong forward bias).

II. DEVICE STRUCTURE AND OPERATION PRINCIPLE

Figure 1 shows the schematic band diagram of the device under consideration. The device comprises the b-As_{1-x}P_xL-GL heterostructure playing the role of the THz active region (THz-AR) mounted on the top of the P⁺-i-N⁺ heterostructure serving as an LED. The THz-AR and LED are separated by a wide-gap transparent barrier layer (TBL). The NIR/MIR radiation (with the photon energy $\hbar\Omega \gtrsim \Delta_{LED}$) generated by the LED passes the TBL and produces the electrons and holes in the b-As_{1-x}P_xL (with the initial kinetic energy $(\varepsilon_0 = \hbar\Omega - \Delta_G)/2$). Since the energy gap, Δ_{LED} is markedly larger than the energy gap Δ_G , in the b-As_{1-x}P_xL, the photogenerated carriers in the latter are fairly hot $\varepsilon_0 \gg k_B T_0$, where k_B and T_0 are the Boltzmann constant and the ambient lattice temperature). If the thickness, d , of the b-As_{1-x}P_xL substantially exceeds the characteristic cooling length l_ε (the carrier energy relaxation length), the photogenerated carriers arrive at the GL being efficiently cooled down the energy $3k_B T_0/2$. Hence, the electron-hole pairs photogenerated in b-As_{1-x}P_xL are injected into the GL having the net energy $\varepsilon_i = \Delta_G + 3k_B T_0$. If $\Delta_{LED} \sim 1$ eV, $\varepsilon_i \ll \Delta_{LED}$.

The cap layer is intended to preserve the GL or it can be a part of THz waveguide. The GL on the device top can be covered by a polycrystalline or by an organic polymer dielectric layer [33]. The top layer can be also made of different materials, for example, from hexagonal boron nitride (hBN). This material can provide the enhanced dynamic properties of the carriers in the GL beneficial for achieving the negative THz conductivity. However, the interaction of the carriers with the interfacial optical phonons can lead to a complex pattern of the interband

and intraband relaxation processes in the GLS [34, 35].

Below we consider the laser heterostructure with the GL active region pumped by the injection of the electron-hole pairs into the absorption-cooling the b-As_{1-x}P_x layer (b-As_{1-x}P_xL) with a small phosphorous content x

It is assumed that the thickness, d , and the absorption coefficient, β_Ω , of the NIR/MIR radiation with the energy $\hbar\Omega > \Delta_G$ in b-As_{1-x}P_xL satisfy the following condition:

$$\beta_\Omega^{-1}, l_\varepsilon \ll d < l_D. \quad (1)$$

Here l_ε is the characteristic length of the carrier energy relaxation (cooling) and l_D is the carrier ambipolar diffusion across the absorption layer. Since the energy relaxation time of the carriers photoexcited in the absorption layer $\tau_\varepsilon = \tau_\varepsilon|_{\varepsilon=(\hbar\Omega-\Delta_G)/2}$ can be assumed to be much shorter than the recombination time τ_R , the ratio $l_\varepsilon/l_D \simeq \sqrt{\tau_\varepsilon/\tau_R} \ll 1$. For the photon energy $\hbar\Omega$, the absorption coefficient can be set as $\beta_\Omega \sim 10^5 \text{ cm}^{-1}$. Hence, for $d \gtrsim 1 \text{ }\mu\text{m}$, inequality (1) should be valid.

According to inequality (1), the generation of the electron-hole pairs by the pumping radiation and their cooling occur primarily close to the irradiated surface of the absorption layer ($z = 0$, the axis z is directed perpendicular to the absorption layer and the GL plane). Therefore, the electron-hole density n in the latter layer obeys the diffusion equation:

$$-D_0 \frac{d^2 n}{dz^2} + \frac{n}{\tau_R} = \beta_\Omega I_\Omega \exp(-\beta_\Omega z). \quad (2)$$

The boundary conditions for Eq. (2) are as follows:

$$D_0 \frac{dn}{dz} \Big|_{z=0} = 0, \quad -D \frac{dn}{dz} \Big|_{z=d} = C_{GL} n|_{z=d}, \quad (3)$$

Here D_0 and τ_R are the coefficient of the carrier ambipolar diffusion perpendicular to the absorption layer and their recombination time at the lattice temperature T_0 , respectively, I_Ω is the photon flux incident on the absorption layer, and C_{GL} is the rate of the carrier capture into the GL (the capture velocity [36, 37]). Introducing the external quantum efficiency of the LED η_Ω one can express I_Ω via the electric power P_{LED} consuming by the LED: $I_\Omega = \eta_\Omega P_{LED}/A\hbar\Omega$, where A is the area of the LED and GL.

The flux of the electrons and holes, J , injected into the GL (captured by the GL) and the flux of the energy, Q , brought by the injected carriers to the 2D-EHP are equal to, respectively,

$$J = -D_0 \frac{dn}{dz} \Big|_{z=d}, \quad Q = -\varepsilon_i D_0 \frac{dn}{dz} \Big|_{z=d}, \quad (4)$$

where $\varepsilon_i = \Delta_G + 3k_B T_0$ and k_B is the Boltzmann constant.

Solving Eq.(2) with boundary conditions (3) and using Eq. (4), we obtain

$$J = \frac{I_\Omega C_{GL}}{(D_0/l_D) \sinh(d/l_D) + C_{GL} \cosh(d/l_D)}, \quad (5)$$

$$Q = \varepsilon_i J, \quad (6)$$

where $l_D = \sqrt{D\tau_R}|_{T=T_0}$ is the carrier ambipolar diffusion length. Equations (5) and (6) are valid if the carriers are photogenerated and cooled down in a narrow layer adjacent to the absorption layer surface (as assumed in line with left-side of inequality (1)).

Since the carrier density in the GL under the laser operation conditions should be sufficiently large (to provide the 2D-EHP degeneration), the inter-carrier collisions, characterized by a short carrier scattering time τ_{cc} could lead to a "Fermitization" of the distribution functions with the common effective temperature $T_e = T_h = T$. Hence, the latter can be presented as $f_e(\varepsilon_h) = [\exp(\varepsilon_e - \mu_e)/k_B T + 1]^{-1}$ and $f_h(\varepsilon_h) = [\exp(\varepsilon_h - \mu_h)/k_B T + 1]^{-1}$, where $\varepsilon_e, \varepsilon_h, \mu_e$, and μ_h are the electron and hole energies and the electron and hole quasi-Fermi energies counted from the Dirac point in the GL.

The quantity C_{GL} depends on the electron and hole densities in the GL. The capture of the photogenerated carriers propagating across the absorption layer is accompanied by the emission of optical phonons and inter-carrier scattering. An increase in the 2D-EHP density in the GL and, hence, an increase in the quasi-Fermi energies $\mu_e + \mu_h$, leads to a decrease of the capture. To account for this effect, we set

$$C_{GL} = C_0 \Theta \left(\frac{\Delta_G - \mu_e - \mu_h}{\Delta_G} \right). \quad (7)$$

Here C_0 is the capture velocity into the empty GL and $\Theta(\delta) = \delta \cdot \theta(\delta)$, where $\theta(\delta)$ is the Heaviside step function ($\theta(\delta) = 1$ if $\delta \geq 0$ and $\theta(\delta) = 0$ if $\delta < 0$). For the heterostructures with the same electron and hole parameters ($\Delta_C = \Delta_V = \Delta_G/2$), considered in the following, one can put $\mu_e = \mu_h = \mu$. In this case, from Eqs. (5) and (7) we obtain

$$J = I_\Omega \frac{\Theta \left(\frac{\Delta_G - 2\mu}{\Delta_G} \right)}{\left[S_0 \sinh \left(\frac{d}{l_D} \right) + \cosh \left(\frac{d}{l_D} \right) \Theta \left(\frac{\Delta_G - 2\mu}{\Delta_G} \right) \right]}, \quad (8)$$

where $S_0 = D_0/C_0 l_D$ is the parameters characterizing the carrier capture into the GL.

III. BALANCE EQUATIONS

The intersubband and intraband carrier relaxation in the GLs under pumping is primarily determined by

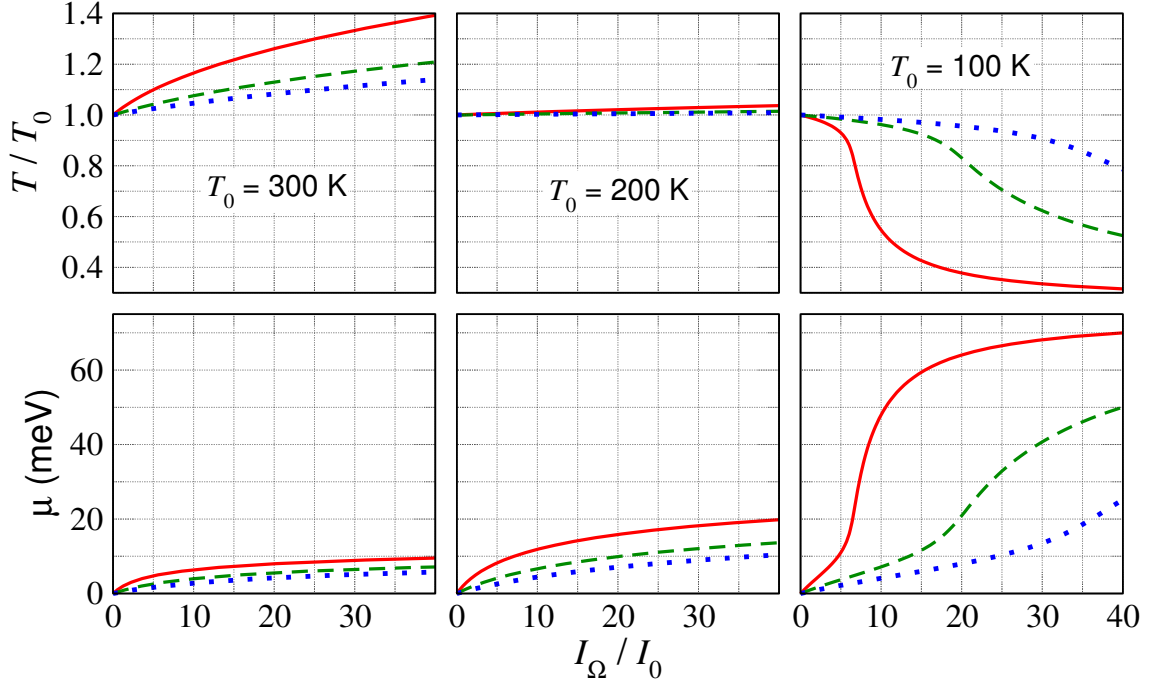


FIG. 2: Normalized effective temperature T/T_0 and quasi-Fermi energy μ versus I_Ω/I_0 calculated for different values of parameter S_0 ($S_0 = 1$ -solid lines, $S_0 = 5$ -dashed lines, and $S_0 = 10$ -dotted lines) and lattice temperatures: $T_0 = 300$ K, $T_0 = 200$ K, and $T_0 = 100$ K.

the interaction with the GL optical phonons [38] (see also, [7, 9, 10, 22]. The direct Auger processes in the GLs are virtually prohibited [39, 40] due to the linear carrier energy spectra [1]. Even though more complex Auger processes can contribute to the interband carrier balance [39–41], we disregard these processes. Considering that in each act of the interband and intraband emission/absorption of the GL optical phonons the 2D-EHP energy decreases/increases by the quantity $\hbar\omega_0$, we present the equation governing the energy balance as [11, 22]

$$\exp\left(\frac{2\mu}{k_B T}\right) \exp\left[\hbar\omega_0 k_B \left(\frac{1}{T_0} - \frac{1}{T}\right)\right] - 1 + a \left\{ \exp\left[\hbar\omega_0 k_B \left(\frac{1}{T_0} - \frac{1}{T}\right)\right] - 1 \right\} = \frac{J}{I_0} \left(\frac{\varepsilon_i}{\hbar\omega_0}\right). \quad (9)$$

The interband balance of electrons and holes is described by

$$\exp\left(\frac{2\mu}{k_B T}\right) \exp\left[\hbar\omega_0 k_B \left(\frac{1}{T_0} - \frac{1}{T}\right)\right] - 1 = \frac{J}{I_0}. \quad (10)$$

Here $I_0 = \Sigma_0/\tau_{Opt}^{inter}$ is the rate of the electron-hole pairs generation due to the absorption of the thermal equilibrium optical phonons with the lattice temperature T_0 , Σ_0 is the characteristic carrier density determined by the energy dependence of the density of state in the GL near the Dirac point, $a = \tau_{Opt}^{inter}/\tau_{Opt}^{intra}$ is the ratio of the pertinent

times characterizing the interband transitions, τ_{Opt}^{inter} and τ_{Opt}^{intra} are the characteristic recombination and intraband relaxation times associated with the carrier interaction with the optical phonons ($\tau_{Opt}^{inter} < \tau_{Opt}^{intra}$ [22]) with $\tau_{Opt}^{intra} \sim \tau_0 \exp(\hbar\omega_0/k_B T_0)$ being larger than the characteristic time of the optical phonon spontaneous emission τ_0 (which is shorter than 1 ps) by a large factor of $\exp(\hbar\omega_0/k_B T_0)$. At $T_0 = 300$ K and $T_0 = 100$ K, one can set [22, 38] $I_0 \sim 10^{21} \text{ cm}^{-2}\text{s}^{-1}$ and $I_0 \sim 10^{14} \text{ cm}^{-2}\text{s}^{-1}$.

The left-hand sides of Eqs. (9) and (10) correspond to the processes of the interband and intraband energy relaxation and the recombination-generation processes. The right-hand sides of these equations represent the energy and carrier fluxes into the GL normalized by I_0 .

IV. CARRIER EFFECTIVE TEMPERATURE AND QUASI-FERMI ENERGIES VERSUS PUMPING

Equations (9) and (10) yield

$$T = \frac{T_0}{1 - \frac{T_0}{\hbar\omega_0} \ln \left[1 + \frac{J}{I_0} \left(\frac{\Delta_G + 3k_B T_0}{\hbar\omega_0} - 1 \right) \frac{1}{a} \right]}, \quad (11)$$

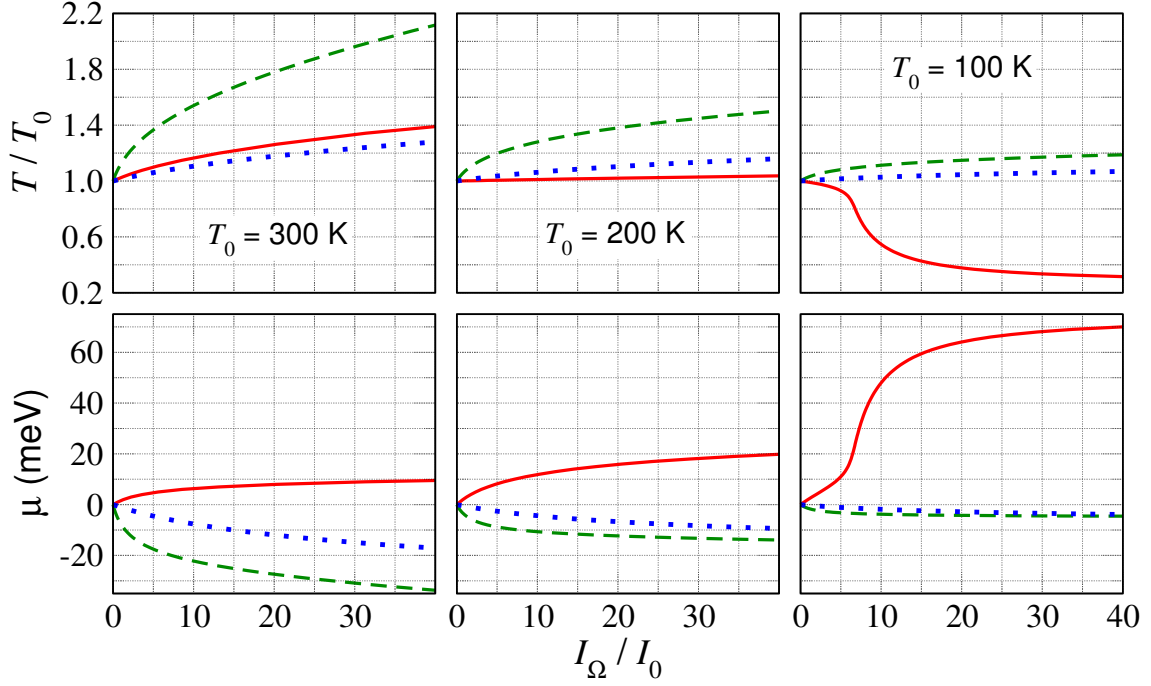


FIG. 3: Normalized effective temperature T/T_0 and quasi-Fermi energy μ as functions of I_Ω/I_0 for the devices with a narrow-gap absorbing-cooling layer (b-AsL) - solid lines, with a wide-absorbing layer (b-PL) - dashed lines, and with direct optical pumping of the GL ($\hbar\Omega = 0.36$ meV) - dotted lines at $T_0 = 300$ K, $T_0 = 200$ K, and $T_0 = 100$ K (for $S_0 = 1$).

$$\frac{\mu}{T} = \frac{1}{2} \ln \left[\frac{1 + \frac{J}{I}}{1 + \frac{J}{I_0} \left(\frac{\Delta_G + 3k_B T_0}{\hbar\omega_0} - 1 \right) \frac{1}{a}} \right]. \quad (12)$$

Equation (11) and (12) together with Eq. (8) describe the variation of the carrier effective temperature and quasi-Fermi energy.

In particular, at the lattice temperature $T_0 = T_0^* = (\hbar\omega_0 - \Delta_G)/3 \simeq 0.05$ eV ($T_0^* \simeq 200$ K), Eqs. (11) and (12) yield $T = T_0^* = \text{const}$.

In line with the experimental data related to the b-P [42] for the carrier mobility in the direction perpendicular to the atomic sheets in the b-As_{1-x}P_x at the temperatures about the room temperature one can set $b \sim 400$ cm²/V·s. This gives $D_0 \sim 10$ cm²/s. Considering that the carrier lifetime in similar material is about $\tau_R \gtrsim 400$ ps [43], we find $l_D \gtrsim 0.6$ μm. The capture velocity can be estimated in the range [36, 37] $C_0 \sim 10^4 - 10^5$ cm/s. As a result, assuming that $d \simeq l_D \simeq 1$ μm, one can find $S_0 \simeq 1 - 10$.

Figure 2 shows the effective temperature T normalized by the lattice temperature T_0 and the quasi-Fermi energy μ calculated using Eqs. (8), (11), and (12) as functions of the normalized pumping intensity $I_\Omega/I_0 \propto P_{LED}$ for $d = l_D$ and different values of parameter $S_0 = D_0/C_0 l_D = 1 - 10$ in the lattice temperatures range $T_0 = 100 - 300$ K. It is assumed that $\Delta_G = 0.150$ eV and $\hbar\omega_0 = 0.2$ eV.

As seen from Fig. 2, the T/T_0 versus I_Ω/I_0 dependences for different lattice temperatures are qualitatively different: at $T_0 = 300$ K, $T_0 = 200$ K, and $T_0 = 100$ K these dependences are rising (the heating of the 2D-EHP), constant (the effective temperature virtually does not change), and decreasing (the cooling of the 2D-EHP), respectively. These distinctions are associated with the difference in the ratio of the power injected by the carriers into the GL and removed by the optical phonons, determined by the quantity $\varepsilon_i/\hbar\omega_0$. Indeed, at $T_0 = 300$ K, $\varepsilon_i = 0.225$ eV, i.e., $\varepsilon_i > \hbar\omega_0$. On the contrary, at $T_0 = 100$ K, $\varepsilon_i = 0.175$ eV corresponding to $\varepsilon_i < \hbar\omega_0$. While in the first case, the injection of the electron-hole pair into the GL increases the 2D-EHP energy by the value $\varepsilon_i - \hbar\omega_0 \simeq 0.025$ eV, in the second case the 2D-EHP energy decreases (by the value $\hbar\omega_0 - \varepsilon_i \simeq 0.025$ eV). When $T_0 = T_0^* = 200$ K, the effective temperature is constant coinciding with T_0 .

At all lattice temperatures under consideration, the quasi-Fermi energy μ increases with increasing I_Ω/I_0 . This increase, being moderate at $T_0 = 300$ K, becomes very steep at $T_0 = 100$ K, so that the pumping efficiency $\propto \mu/I_\Omega$ could be large.

One needs to point out that the plots related to the different lattice temperatures correspond fairly different values of I_Ω because of a strong dependence of I_0 on T_0 (see the above estimates for I_0). This, in particular, implies that at $T_0 = 100$ K a significant change in T/T_0 and μ can be achieved at the photon flux I_Ω much smaller (by several orders of magnitude) than at $T_0 = 300$ K.

Thus, a decrease of T_0 is an important factor for the enhancement of the pumping efficiency.

Figure 3 compares the pumping efficiency of the proposed laser heterostructure with the absorption-cooling narrow-gap layer (b-AsL, $x = 0$) and of the device having a wide-gap absorbing layer (b-PL, $x = 1$ and $\Delta_G = 0.3$ eV) - both with $S_0 = 1$, as well the GL-based heterostructure with the direct optical pumping of the GL without the absorbing layer (see Appendix A). We assumed that all the devices under comparison are irradiated by a MIR laser such as having the InAs active region, setting $\hbar\Omega = 0.36$ meV. The coefficient of the pumping radiation absorption in the GL is $\beta = 0.023$. As seen from Fig. 3, in the case of the absence of the preliminary carrier cooling in the absorbing layer and $\Delta_G = 0.3$ eV, a strong increase in the effective temperature leads to $\mu < 0$, i.e., to the 2D-EHP nondegeneracy. The same occurs in the case of the direct pumping with $\hbar\Omega = 0.36$ meV. The suppression of the population inversion despite an increase in the carrier density in the GL is, in this particular case, associated with an excessive rise of the effective temperature.

In contrast, the loss of the carrier energy in the absorption-cooling layer can lead to a moderate increase in T with increasing I_Ω at $T_0 = 300$ K, to an insensitivity of T to I_Ω at $T_0 = 200$ K, and even to a marked drop of T at $T_0 = 100$ K. The latter implies that pumping results in the 2D-EHP cooling. In all these cases, μ exhibits an increase, which is particularly steep at $T_0 = 100$ K, corresponding to a strong 2D-EHP degeneracy and population inversion.

When the energy of the pumping photons $\hbar\Omega > 2\hbar\omega_0$, the situation can be different, i.e., the population inversion in the devices without carrier cooling in the absorption layer and in the devices with the direct optical pumping can be also achieved. At such photon energies, that the carriers injected from the absorbing layer with $\Delta_G \lesssim \hbar\Omega$ into the GL and the carriers directly photogenerated in the GL might emit a cascade of the optical phonons before the carrier Fermitization. This requires that the time, τ_0 , of the spontaneous emission of the optical phonons in the GL should be sufficiently short in comparison with the inter-carrier collision time τ_{cc} . At the pumping by the high energy photons, the mutual collisions of the photogenerated carriers having relatively high energy can be characterized by not too short τ_{cc} . In this case, the effective initial energy of the electron-hole pair in the GL can be estimated as $\varepsilon_i^{eff} = \hbar\Omega - 2K\hbar\omega_0/(1 + K\tau_0/\tau_{cc})$ [22] (see also Appendix A), where K is the number of the optical phonons which can be emitted by the carrier injected into the GL. Considering this situation, from Eqs. (A3) and (A4) one can find that the following three cases can be realized:

(a) $a < \frac{\Omega}{\omega_0} - 1 - \frac{2K}{1 + K(\tau_0/\tau_{cc})}$, corresponding to $dT/dI_\Omega > 0$ (carrier heating) and $d\mu/dI_\Omega < 0$ ($\mu < 0$, hence, no population inversion);

(b) $0 < \frac{\Omega}{\omega_0} - 1 - \frac{2K}{1 + K(\tau_0/\tau_{cc})} < a$, corresponding to $dT/dI_\Omega > 0$ (carrier heating) and $d\mu/dI_\Omega > 0$ ($\mu > 0$, population inversion);

(c) $\frac{\Omega}{\omega_0} - 1 - \frac{2K}{1 + K(\tau_0/\tau_{cc})} < 0$, corresponding to $dT/dI_\Omega < 0$ (carrier cooling) and $d\mu/dI_\Omega > 0$ ($\mu > 0$, population inversion).

The population inversion in the 2D-EHP accompanied by its the cooling occurs, for example, in the case of direct optical pumping by a CO₂ laser ($\hbar\Omega \sim 0.1$ eV, so that the latter inequality is satisfied ($K = 0$ and $\Omega/\omega_0 - 1 \simeq -0.5$). In particular, if $\Omega/\omega_0 = 2 + \delta$ with $\delta < 1$, $K = 1$, and the condition of both cooling and population inversion at the direct optical pumping can be presented as $\tau_0/\tau_{cc} < (1 - \delta)/(1 + \delta)$.

V. DYNAMIC CONDUCTIVITY AND THZ AMPLIFICATION

The contributions of the direct interband optical transitions to the real part of the 2D-EHP dynamic conductivity $\text{Re}\sigma_\omega^{inter}$ can be found as in the previous papers [9–12] (see also Refs. [7, 45–47]):

$$\text{Re}\sigma_\omega^{inter} \simeq \frac{e^2}{4\hbar} \tanh\left(\frac{\hbar\omega - 2\mu}{4k_B T}\right). \quad (13)$$

One can see that in the range $\hbar\omega < 2\mu$, $\text{Re}\sigma_\omega^{inter} < 0$. This implies that the 2D-EHP can serve as an active region for the amplification of the photonic or surface plasmon modes propagating along the GL and their lasing. However, the spectral range where $\text{Re}\sigma_\omega^{inter} < 0$ is limited by not too large $\hbar\omega > \hbar\omega_D \sim \hbar/\tau$ by the carrier intraband absorption (the Drude absorption). In reality, the value $\hbar\omega_D$, which is primarily determined by the carrier momentum relaxation time τ_p ($\omega_D \sim D/2\pi\tau$) in the GL, can be much smaller than 2μ . At $\tau_p \sim 1 - 3$ ps, the absolute value of the dynamic conductivity for $\hbar\omega \sim 10 - 30$ meV can be only slightly smaller than $e^2/4\hbar$. In this case, the surface plasmon amplification coefficient can be fairly large (about $\alpha_\omega \sim 10^4$ cm⁻¹).

The carriers in the absorbing-cooling layer, particularly, in a narrow vicinity of the GL can lead to an increase in the "parasitic" absorption of the THz radiation emitted by the laser heterostructure at the population inversion in the GL. Therefore, the carrier density in this region $n_{GL} \simeq n|_{z=d-0}$ should be limited. This density can be estimates as

$$n_{GL} = \frac{J}{C_{GL}} = \frac{n_0}{\left[S_0 \sinh\left(\frac{d}{l_D}\right) + \cosh\left(\frac{d}{l_D}\right) \Theta\left(\frac{\Delta_G - 2\mu}{\Delta_G}\right) \right]} \frac{I_\Omega}{I_0}, \quad (14)$$

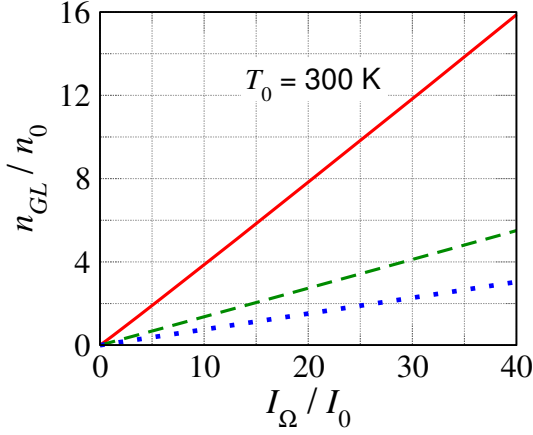


FIG. 4: Normalized carrier density in the absorption layer n_{GL}/n_0 versus I_Ω/I_0 at $T_0 = 300$ K calculated for and different values of S_0 : $S_0 = 1$ -solid line, $S = 5$ -dashed line, and $S_0 = 10$ - dotted line.

where $n_0 = I_0/C_0$. At $T_0 = 300$ K setting $C_0 = (10^4 - 10^5)$ cm/s, one obtains $n_0 \sim (10^{16} - 10^{17})$ cm $^{-3}$.

Figure 4 shows the normalized carrier density n_{GL}/n_0 as a function of the normalized pumping intensity I_Ω/I_0 calculated for $T_0 = 300$ K and different values of S_0 (other parameters are the same as for Fig. 2).

These values of the absorption coefficient mentioned above, are markedly higher than the absorption coefficient, $-\alpha_\omega^{a-c}$, associated with the free carrier absorption in the absorbing-cooling layer near the GL where the plasmons are located. (in the direction perpendicular to the GL plane) [35]. At $n_{GL} \simeq n_0 \simeq (10^{16} - 10^{18})$, i.e., at the values corresponding to Fig. 4, one obtains $\alpha_\omega^* \simeq 3 \times (10 - 1000)$ cm $^{-1}$, i.e., $\alpha_\omega^* \ll \alpha_\omega$.

VI. DISCUSSION

Apart from this, The recombination and the intraband energy relaxation lead to the generation of nonequilibrium (hot) optical phonons in the GL (heating of the optical phonon system). This system cools down through anharmonic decay to acoustic phonons which are subsequently absorbed into the substrate [33, 48–50]. However, it was shown experimentally, that the optical phonon decay time in the GL-heterostructures, in particular, the GL-hBN heterostructures is estimated to be about [33] $\tau_{Opt}^{decay} \sim 0.200 - 0.375$ ps. At such decay times, the deviation of the optical phonon system from equilibrium is insignificant. This implies that this system temperature is close to the equilibrium temperature T_0 . In particular, in the case of the heterostructures with, in particular, the hBN top layer, due to the large specific heat capacity of this layer, the rise of the lattice temperature even under relatively strong pumping is small (~ 1 K) [33].

The carriers generated in the absorption-cooling layer transfer their excessive energy to the lattice of this layer.

The heating of this layer can lead to an increase in T_0 if the heat drain is insufficient. From the above results we can see that at lowered lattice temperatures, a sufficiently strong population inversion (a large ratio μ/T can be achieved at moderate photon fluxes of the pumping radiation and, hence, using not so powerful LEDs. In this case, the device heating might be weak. At elevated lattice temperatures, the heat power generated in the device can be substantial despite high heat conductivity of the materials in the device in question (in particular, the GLs). This might necessitate using special device configurations promoting an effective heat removal of work in the pulse regime. The devices with the absorption-cooling layer proposed and considered by us can demonstrate higher pumping efficiency in comparison that with the absorption layer [21]. However, both devices exhibit the same lattice heating provided the same pumping photon energy and flux. The point is that the excessive photon energy converts into the lattice heat in the absorbing-cooling layer in the former device, while this energy goes directly to the 2D-EHP (resulting in its stronger heating) in the GL in the latter.

The possibility to enhance the pumping efficiency of in the heterostructure under consideration is associated with a relatively low energy gap in the absorbing-cooling layer and the proper band alignment of this layer material and the GLs. In principle, other narrow-gap materials can be used.

We considered the device in which the pumping source (LED) is integrated into the device structure. Naturally, the GL-based heterostructures with b-As $_{1-x}$ P $_x$ L or similar absorbing-cooling layer with the optical pumping by separate sources can be used for the THz lasing.

To realize a practical laser device with the proposed heterostructure a pertinent laser cavity with good mode-field confinement needs to be integrated. The THz photon generation due to the transitions in the GLs includes both the in-plane and vertical modes. As is similar to a vertical cavity surface emitting laser diode, a Fabry-Perot vertical cavity might be implemented along with the substrate (with a back-side full-reflection mirror coat and a top-side high reflection mirror coat). Also analogously to an edge-mode laser diode a distributed feedback cavity as well as a distributed bragg reflector cavity can be implemented.

Conclusion

We propose to use a b-As $_{1-x}$ P $_x$ L-GL heterostructure integrated with a NIR/MIR LED as an active region for the terahertz lasers. the b-As $_{1-x}$ P $_x$ L sandwiched between the LED and GL serves for the LED radiation absorption, the carrier generation and cooling followed by their injection. Using the b-As $_{1-x}$ P $_x$ LS, exhibiting narrow energy gaps, enables the injection of relatively cool carriers. This provides a higher pumping efficiency in comparison with the laser GL-based heterostructures

with relatively wide-gap absorbing layer and the laser GL-based heterostructures with the direct optical pumping. We demonstrated that in the devices with p-AsL ($x \simeq 0$), i.e., with the absorbing-cooling layer characterized by the energy gap smaller than the GL-optical phonon energy, the carrier effective temperature in the GL can become lower than the lattice temperature. This might result in a further enhancement of the pumping efficiency and the THz laser performance.

The authors are grateful to V. Ya. Aleshkin and A. A. Dubinov for useful data related to the surface plasmon absorption by the free carriers in the absorbing-cooling layer.

The work at RIEC and UoA was supported by Japan Society for Promotion of Science (Grants Nos. 16H-06361 and 16K-14243), the works at MIPT and RPI were supported by Russian Foundation for Basic Research (Grant Nos. 18-29-02089 and 18-07-01379) and by Office of Naval Research (Project Monitor Dr. Paul Maki), respectively.

Appendix A. Direct optical pumping

In the case of the direct pumping of the GL by the LED NIR/MIR radiation, Eqs. (5), (9), and (10) should be replaced by the following [22]:

$$\exp\left(\frac{2\mu}{k_B T}\right) \exp\left[\hbar\omega_0 k_B \left(\frac{1}{T_0} - \frac{1}{T}\right)\right] - 1 + a \left\{ \exp\left[\hbar\omega_0 k_B \left(\frac{1}{T_0} - \frac{1}{T}\right)\right] - 1 \right\} = \beta \frac{I_\Omega}{I_0} \left(\frac{\varepsilon_i^{eff}}{\hbar\omega_0}\right), \quad (A1)$$

$$\exp\left(\frac{2\mu}{k_B T}\right) \exp\left[\hbar\omega_0 k_B \left(\frac{1}{T_0} - \frac{1}{T}\right)\right] - 1 = \beta \frac{I_\Omega}{I_0}. \quad (A2)$$

Here $\beta = 0.023$, $\varepsilon_i^{eff} = \hbar\Omega - b\hbar\omega_0$, where $b = 2K/(1 + K\tau_0/\tau_{cc})$, K is the number of optical phonons in their cascade in the GL, and τ_0 and τ_{cc} were defined above.

Solving Eqs. (A1) and (A2), we obtain

$$\frac{T}{T_0} = \frac{1}{1 - \frac{k_B T_0}{\hbar\omega_0} \ln \left[1 + \frac{\beta}{a} \frac{I_\Omega}{I_0} \left(\frac{\Omega}{\omega_0} - b - 1 \right) \right]} \simeq \left(\frac{k_B T_0}{\hbar\omega_0} \right) \left(\frac{\beta}{a} \right) \left(\frac{\Omega}{\omega_0} - b - 1 \right) \frac{I_\Omega}{I_0}, \quad (A3)$$

$$\frac{\mu}{T} = \frac{1}{2} \ln \left[\frac{1 + \beta \frac{I_\Omega}{I_0}}{1 + \frac{\beta}{a} \left(\frac{\Omega}{\omega_0} - b - 1 \right) \frac{I_\Omega}{I_0}} \right] \simeq \frac{\beta}{2} \left[1 - \frac{1}{a} \left(\frac{\Omega}{\omega_0} - b - 1 \right) \frac{I_\Omega}{I_0} \right]. \quad (A4)$$

-
- [1] A. H. Castro Neto, F. Guinea, N. M. R. Peres, K.S. Novoselov, and A. K. Geim, "The electronic properties of graphene," *Rev. Mod. Phys.*, vol. 81, pp. 109–162, 2009.
 - [2] F. Bonaccorso, Z. Sun, T. Hasan, and A. C. Ferrari. "Graphene photonics and optoelectronics," *Nat. Photon.* vol. 4: pp. 611–622 2010.
 - [3] V. Ryzhii, N. Ryabova, M. Ryzhii, N. V. Baryshnikov, V. E. Karasik, V. Mitn, and T. Otsuji. "Terahertz and infrared photodetectors based on multiple graphene layer and nanoribbon structures," *Opto-Electron. Rev.* vol. 20, pp. 15–20 2012.
 - [4] Q. Bao and K. P. Loh, "Graphene photonics, plasmonics, and broadband optoelectronic devices," *ACS Nano* vol. 6, pp. 3677–3677, 2012.
 - [5] A. Tredicucci and M. S. Vitiello, "Device concepts for graphene-based terahertz photonics," *IEEE J. Sel. Top. Quantum Electron.* vol. 20, p. 8500109, 2014.
 - [6] F. H. L. Koppens, T. Mueller, Ph. Avouris, A. C. Ferrari, M. S. Vitiello, and M. Polini. "Photodetectors based on graphene, other two-dimensional materials and hybrid systems," *Nat. Nanotech.* vol. 9, pp. 780–793 2014.
 - [7] V. Ryzhii, M. Ryzhii, and T. Otsuji, "Negative dynamic conductivity of graphene with optical pumping," *J. Appl. Phys.* vol. 101, pp. 083114-1–083114-4 2007.
 - [8] M. Ryzhii and V. Ryzhii, "Injection and population inversion in electrically induced pn junction in graphene with split gates," *Jpn. J. Appl. Phys.* vol. 46, pp. L151–L153 2007.
 - [9] V. Ryzhii, M. Ryzhii, A. Satou, T. Otsuji, A. A. Dubinov, and V. Y. Aleshkin, "Feasibility of terahertz lasing in optically pumped epitaxial multiple graphene layer structures," *J. Appl. Phys.* vol. 106, pp. 084507-1–084507-6 2009.
 - [10] V. Ryzhii, A. A. Dubinov, T. Otsuji, V. Mitin, M. S. Shur, "Terahertz lasers based on optically pumped multiple graphene structures with slot-line and dielectric waveguides," *J. Appl. Phys.* vol. 107, pp. 054505-1–054505-5 2010.
 - [11] V. Ryzhii, M. Ryzhii, V. Mitin, and T. Otsuji, "Toward the creation of terahertz graphene injection laser," *J. Appl. Phys.* vol. 110, pp. 094503-1–094503- 2011.
 - [12] A. A. Dubinov, V. Ya. Aleshkin, V. Mitin, T. Otsuji, and V. Ryzhii, "Terahertz surface plasmons in optically pumped graphene structures," *J. Phys.: Cond. Mat.* vol. 23, p. 145302 2011.
 - [13] V. V. Popov, O. V. Polischuk, A. R. Davoyan, V. Ryzhii, T. Otsuji, and M. S. Shur, "Plasmonic terahertz lasing in an array of graphene nanocavities," *Phys. Rev. B* vol.

- 86, p. 195437 2012.
- [14] S. Boubanga-Tombet, S. Chan, T. Watanabe, A. Satou, V. Ryzhii, and T. Otsuji, "Ultrafast carrier dynamics and terahertz emission in optically pumped graphene at room temperature," *Phys. Rev. B* vol. 85, p. 035443, 2012.
 - [15] T. Li, L. Luo, M. Hupalo, J. Zhang, M. C. Tringides, J. Schmalian, and J. Wang, "Femtosecond population inversion and stimulated emission of dense Dirac fermions in graphene," *Phys. Rev. Lett.* vol. 108, p. 167401, 2012.
 - [16] I. Gierz, J. C. Petersen, M. Mitrano, C. Cacho, I. E. Turcu, E. Springate, A. Stohr, A. Kohler, U. Starke, and A. Cavalleri, "Snapshots of non-equilibrium Dirac carrier distributions in graphene," *Nat. Mater.* vol. 12, pp. 1119–1124, 2013.
 - [17] T. Watanabe, T. Fukushima, Y. Yabe, S. A. Boubanga-Tombet, A. Satou, A. A. Dubinov, V. Ya. Aleshkin, V. Mitin, V. Ryzhii, and T. Otsuji, "The gain enhancement effect of surface plasmon-polaritons on terahertz stimulated emission in optically pumped monolayer graphene," *New J. Phys.* vol. 15, p. 07503, 2013.
 - [18] T. Otsuji, T. S. B. Tombet, A. Satou, M. Ryzhii, and V. Ryzhii, "Terahertz wave generation using graphene: toward new types of terahertz lasers" *IEEE J. Sel. Top. Quantum Electron.* vol. 19, No. 1, p. 8400209 2013.
 - [19] D. Yadav, S. Boubanga Tombet, T. Watanabe, S. Arnold, V. Ryzhii, and T. Otsuji, "Terahertz wave generation and detection in double-graphene layered van der Waals heterostructures," *2D Materials* vol. 2, p. 045009 2016.
 - [20] D. Yadav, G. Tamamushi, T. Watanabe, J. Mitsushio, Y. Tobah, K. Sugawara, A. A. Dubinov, A. Satou, M. Ryzhii, V. Ryzhii, and T. Otsuji, "Terahertz light-emitting graphene-channel transistor toward single-mode lasing," *Nanophotonics* vol. 7, pp. 741–752 2018.
 - [21] A. R. Davoyan, M. Yu. Morozov, V. V. Popov, A. Satou, and T. Otsuji, "Graphene surface emitting terahertz laser: diffusion pumping concept," *Appl. Phys. Lett.* vol. 103, p. 251102, 2013.
 - [22] V. Ryzhii, M. Ryzhii, V. Mitin, A. Satou, and T. Otsuji, "Effect of heating and cooling of photogenerated electron-hole plasma in optically pumped graphene on population inversion," *Jpn. J. Appl. Phys.* vol. 50, pp. 094001-1-094001-9, 2011.
 - [23] Y. Cai, G. Zhang, and Y.-W. Zhang, Layer-dependent band alignment and work function of few-layer phosphorene," *Sci. Reports* vol. 4, 6677 2014.
 - [24] H. Asahina and A. Morita, "Band structure and optical properties of black phosphorus," *J. Phys. C: Solid State Phys.* vol. 17, pp. 1839–1852 1984.
 - [25] Xi Ling, H. Wang, S. Huang, F. Xia, and M. S. Dresselhaus, "The renaissance of black phosphorus," *PNAS* vol. 112, pp. 4523–4530 2015.
 - [26] R. Yan, Q. Zhang, W. Li1, I. Calizo, T. Shen1, C. A. Richter, A. R. Hight-Walker, X. Liang, A. Seabaugh, D. Jena, H. G. Xing, D. J. Gundlach, and N. V. Nguyen, "Determination of graphene work function and graphene-insulator-semiconductor band alignment by internal photoemission spectroscopy," *Appl. Phys. Lett.*, vol. 101, p. 022105, 2012.
 - [27] G. Gong, H. Zhang, W. Wang, L. Colombo, R. M. Wallace, and K. Cho, "Band alignment of two-dimensional transition metal dichalcogenides: Application in tunnel field effect transistors," *Appl. Phys. Lett.*, vol. 103, p. 053513, 2013.
 - [28] B. Liu, M. Kopf, A. N. Abbas, X. Wang, Q. Guo, Y. Jia, F. Xia, R. Wehrich, F. Bachhuber, F. Pielhofer, H. Wang, R. Dhall, S. B. Cronin, M. Ge, X. Fang, T. Nilges, and C. Zhou, "Black Arsenic Phosphorus: layered anisotropic infrared semiconductors with highly tunable compositions and properties," *Adv. Mater.* vol. 27, pp. 4423–4429 2015.
 - [29] M. Long, A. Gao, P. Wang, et al. "Room temperature high-detectivity mid-infrared photodetectors based on black arsenic phosphorus," *Sci. Adv.* vol. 3, no. 6, e1700589, 2017.
 - [30] S. Yuan, C. Shen, B. Deng, et al. "Air-stable room-temperature mid-infrared photodetectors based on hBN/black arsenic phosphorus/hBN heterostructures," *Nano Lett.* vol. 18, pp. 31723179, 2018.
 - [31] Li Yu, Z. Zhu, A. Gao1, J. Wang, F. Miao1, Yi Shi, and X. Wang, "Electrically tunable optical properties of few-layer black arsenic phosphorus," *Nanotechnology* vol. 29, No. 48 2018.
 - [32] Y. Chen, C. Chen, R. Kealhofer, H. Liu, Z. Yuan, L. Jiang, J. Suh, J. Park, C. Ko, H. S. Choe, J. Avila, M. Zhong, Z. Wei, J. Li, S. Li, H. Gao, Y. Liu, J. Analytis, Q. Xia, M. C. Asensio, and J. Wu, "Black Arsenic: a layered semiconductor with extreme inplane anisotropy," *Adv. Mat.* vol. 3, e1800754 2018.
 - [33] V. Sharma, C. Wang, R. G. Lorenzini, R. Ma, Q. Zhu, D. W. Sinkovits, G. Pilania, A. R. Oganov, S. Kumar, G. A. Sotzing, S. A. Boggs, and R. Ramprasad, "Rational design of all organic polymer dielectrics," *Nat. Com.* vol. 5, 4845 2014.
 - [34] D. Golla, A. Brasington, B. J. LeRoy, and A. Sandhu, "Ultrafast relaxation of hot phonons in graphene-hBN heterostructures," *APL Materials* vol. 5, p. 056101 2017.
 - [35] V. Ryzhii, T. Otsuji, M. Ryzhii, A. A. Dubinov, V. Ya. Aleshkin, V. E. Karasik, and M. S. Shur, "Amplification of surface plasmons in graphene-black phosphorus injection laser heterostructures," *arXiv*: 1901.00580.
 - [36] E. Rosencher, B. Vinter, F. Luc, L. Thibaudau, P. Bois, and J. Nagle, "Emission and capture of electrons in multiquantum-well structures," *IEEE Trans. Quantum Electron.* vol. 30, pp. 2975–2888, 1994.
 - [37] V. Ya. Aleshkin, A. A. Dubinov, M. Ryzhii, V. Ryzhii, and T. Otsuji, "Electron capture in van der Waals graphene-based heterostructures with WS₂ barrier layers," *J. Phys. Soc. Jpn.* vol. 84, pp. 094703-1-094703-7, 2015.
 - [38] F. Rana, P. A. George, J. H. Strait, S. Sharavaraman, M. Charasheyhar, and M. G. Spencer, "Carrier recombination and generation rates for intravalley and intervalley phonon scattering in graphene," *Phys. Rev. B* vol. 79, pp. 115447-1-115447-5 2009.
 - [39] M. S. Foster and I. L. Aleiner, "Slow imbalance relaxation and thermoelectric transport in graphene," *Phys. Rev. B* vol. 79, p. 085415 2009.
 - [40] G. Alymov, V. Vyurkov, V. Ryzhii, A. Satou, and D. Svintsov, "Auger recombination in Dirac materials: A tangle of many-body effects," *Phys. Rev. B* vol. 97, p. 205411 2018.
 - [41] V. Ryzhii, D. S. Ponomarev, M. Ryzhii, V. Mitin, M. S. Shur, and T. Otsuji, "Negative and positive terahertz and infrared photoconductivity in uncooled graphene," *Opt. Mat. Exp.* vol. ...pp.... 2019.
 - [42] A. Morita, "Semiconducting Black Phosphorus," *Appl. Phys. A* vol. 39, pp. 227–242 1986.
 - [43] M. Nurmamat, Y. Ishida, R. Yori, K. Sumida, S. Zhu, M.

- Nakatake, Y. Ueda, M. Taniguchi, S. Shin, Y. Akahama, and A. Kimura, "Prolonged photo-carriers generated in a massive-and-anisotropic Dirac material," *Sci. Rep.*, vol. 8, 9073 2018.
- [44] A. Krier, "Physics and technology of mid-infrared light emitting diodes," *Phil. Trans. R. Soc. Lond. A* vol. 359, pp.599-619 2001.
- [45] L. A. Falkovsky and A. A. Varlamov, "Space-time dispersion of graphene conductivity," *European Phys. J. B* vol. 56, pp. 281-289 2007.
- [46] E. H. Hwang, S. Adam, and S. D. Sarma, "Carrier transport in two-dimensional graphene layers," *Phys. Rev. Lett.* vol. 98, p. 186806 2007.
- [47] D. Svintsov, V. Ryzhii, A. Satou, T. Otsuji, and V. Vyurkov, "Carrier-carrier scattering and negative dynamic conductivity in pumped graphene," *Opt. Express* vol. 22, pp. 19873–19886 2014.
- [48] H. Wang, J. H. Strait, P. A. George, S. Shivaraman, V. D. Shields, M. Chandrashekhara, J. Hwang, F. Rana, M. G. Spencer, C. S. Ruiz-Vargas, and J. Park, "Ultrafast relaxation dynamics of hot optical phonons in graphene," *Appl. Phys. Lett.* vol. 96, p. 081917 2010.
- [49] J. M. Iglesias, M. J. Martn, E. Pascual, and R. Rengel, "Hot carrier and hot phonon coupling during ultrafast relaxation of photoexcited electrons in graphene," *Appl. Phys. Lett.* vol. 108, 043105 (2016).
- [50] H. Wang, J. H. Strait, P. A. George, S. Shivaraman, V. D. Shields, M. Chandrashekhara, J. Hwang, F. Rana, M. G. Spencer, C. S. Ruiz-Vargas, et al., "Ultrafast relaxation dynamics of hot optical phonons in graphene," *Appl. Phys. Lett.* vol. 96, pp. 081917-1-081917-4 2010.